Metal boundary modelling for non-orthogonal FDTD

R. Nilavalan [(1)], I. J. Craddock [(2)], M. G. Hadjinicolaou [(1)]

[(1)] Electronic and Computer Engineering, Brunel University, Uxbridge, UB8 3PH, UK,
Rajagopal.Nilavalan@brunel.ac.uk, Marios.Hadjinicolaou@brunel.ac.uk
[(2)] Centre for Communications Research, University of Bristol, Bristol, BS8 1UB, UK,
Ian.Craddock@bristol.ac.uk

Abstract - **This contribution looks into a technique to reduce numerical errors when employing non-orthogonal mesh in modelling curved structures. A novel technique is analysed using microstrip line and a patch antenna and the results are presented.**

I. Introduction

Numerical electromagnetic models, such as Finite-Difference Time-Domain (FDTD), have many applications. This method was originally put forward by K.S.Yee [1] and implemented in Cartesian co-ordinates. However, if the structure being modelled does not align to the orthogonal Cartesian grid, staircasing errors are introduced. To resolve this problem, a number of conformal mesh-based FDTD methods have been developed, such as Contour Path FDTD (CPFDTD)[2], non-orthogonal FDTD [3] and the Discrete Surface Integral (DSI) method. This contribution focuses on the Non-Orthogonal FDTD method. This method is based upon a discretisation of Maxwell's curl equations in local curvilinear co-ordinates on a structured mesh employing covariant and contravariant field components. The Non-Orthogonal FDTD method is very useful in modelling curved structures such as conformal antennas.

Results from numerical electromagnetic analysis methods, such as FDTD technique, are often degraded by an error known as numerical dispersion. A practical guide to the dispersion caused by the use of Non-Orthogonal FDTD meshes was published [4] and subsequent research work revealed that these numerical dispersion errors are higher when modelling metallic boundaries in non-orthogonal FDTD due to the algorithm's reciprocal field interpolation scheme [5].

This paper analyses a technique to reduce numerical errors when employing non-orthogonal mesh in modelling curved structures. A novel technique is analysed using Microstrip line and a patch antenna and the results are presented. The stability issues are also considered carefully when implementing this technique.

II. Modelling Metal Boundaries with Non-Orthogonal Coordinates

Non-Orthogonal FDTD is formulated on a structured grid, described by a local non-orthogonal coordinate system, which is characterised by covariant unit vectors U_1, U_2, U_3 (tangential to the unit cell edges) as shown by Figure 1, and contravariant unit vectors U^1, U^2, U^3 (lying normal to the cell faces).

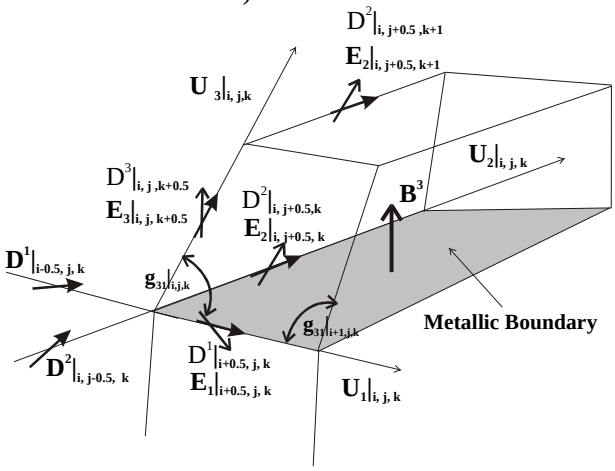

Figure 1: *Location of a metallic boundary in a unit cell.*

The Non-Orthogonal algorithm may be described by a system of matrix-vector equations [6], an iteration step (where new values of contravariant fields are calculated):

$$\frac{\mathbf{D}^{n+1}-\mathbf{D}^{n}}{\Delta t}=\mathbf{C}_h\mathbf{H}^{n+1/2}, \qquad -\frac{\mathbf{B}^{n+1/2}-\mathbf{B}^{n-1/2}}{\Delta t}=\mathbf{C}_e\mathbf{E}^{n} \tag{1}$$

and an interpolation step (yielding covariant components):

$$E_i=\sum_j \frac{\mathbf{U}_i\cdot\mathbf{U}_j}{\varepsilon\sqrt{g}}D^j \Rightarrow \mathbf{E}=\mathbf{M}_\varepsilon\mathbf{D} \tag{2}$$

And similarly,

$$\mathbf{H}=\mathbf{M}_\mu\mathbf{B} \tag{3}$$

Where, **E** and **H** are vectors consisting of all the covariant field values in the algorithm, **B** and **D** are the contravariant components and $\mathbf{C_e}$ and $\mathbf{C_h}$ are matrices that implement the curl operation. $\mathbf{M_\varepsilon}$ and $\mathbf{M_\mu}$ are matrices that describe both material properties and the interpolation that yields the necessary covariant components. $\sqrt{g}$ represents the volume of the cell.

Considering the covariant component $E_1|_{i+0.5,j,k}$ in Figure 1, the interpolation step equation 2, yields:

$$E_1\big|_{i+0.5,j,k} = \frac{\mathbf{U}_1\big|_{i,j,k} \cdot \mathbf{U}_1\big|_{i,j,k}}{\varepsilon\sqrt{g}} D^1\big|_{i+0.5,j,k} + \left\{ \frac{\mathbf{U}_1\big|_{i,j,k} \cdot \mathbf{U}_3\big|_{i,j,k}}{4\varepsilon\sqrt{g}} D^3\big|_{i,j,k+0.5} + \frac{\mathbf{U}_1\big|_{i,j,k} \cdot \mathbf{U}_3\big|_{i+1,j,k}}{4\varepsilon\sqrt{g}} D^3\big|_{i+1,j,k+0.5} + \ldots\ldots\ldots\ldots \right\} \quad (4)$$

Whereas for $E_3|_{i,j,k+0.5}$, the interpolation gives:

$$E_3\big|_{i,j,k+0.5} = \frac{\mathbf{U}_3\big|_{i,j,k} \cdot \mathbf{U}_3\big|_{i,j,k}}{\varepsilon\sqrt{g}} D^3\big|_{i,j,k+0.5} + \left\{ \frac{\mathbf{U}_3\big|_{i,j,k} \cdot \mathbf{U}_1\big|_{i,j,k}}{4\varepsilon\sqrt{g}} D^1\big|_{i+0.5,j,k} + \frac{\mathbf{U}_3\big|_{i,j,k} \cdot \mathbf{U}_1\big|_{i,j,k+1}}{4\varepsilon\sqrt{g}} D^1\big|_{i+0.5,j,k+1} + \ldots\ldots\ldots \right\} \quad (5)$$

For stability [6] the material matrices $\mathbf{M}_\varepsilon$ and $\mathbf{M}_\mu$ must be symmetric, this is achieved as a result of the coupling between components $E_1|_{i+0.5,j,k}$ and $E_3|_{i,j,k+0.5}$, being reciprocal, since:

$$\frac{\mathbf{U}_3\big|_{i,j,k} \cdot \mathbf{U}_1\big|_{i,j,k}}{4\varepsilon\sqrt{g}} = \frac{\mathbf{U}_1\big|_{i,j,k} \cdot \mathbf{U}_3\big|_{i,j,k}}{4\varepsilon\sqrt{g}} \quad (6)$$

However, at a metallic boundary, such as that shown in Figure 1, the tangential electric field $E_1|_{i+0.5,j,k}$ must be zero, and hence the contribution to this component from $E_3|_{i,j,k+0.5}$ ($D^3|_{i,j,k+0.5}$) in equation (4), must be set to zero. However, as a necessary consequence of reciprocity, the contribution from $E_1|_{i+0.5,j,k}$ ($D^1|_{i+0.5,j,k}$) to $E_3|_{i,j,k+0.5}$ in equation (5) must also then be zero (if this is ignored, instability will result).

In effect, therefore, it appears to the model as if $U_3\big|_{i,j,k} \cdot U_1\big|_{i,j,k} = 0$, which is not true - unless the mesh is orthogonal at the boundary. This is an undesirable approximation, which gives rise to additional error in non-orthogonal FDTD. A detailed analysis of this error was presented in [5].

These errors can be reduced if the interpolation step at the metallic boundary is not ignored. If $D^1|_{i+0.5,j,k} \neq 0$ and this field component is calculated in such a way that $E_1|_{i+0.5,j,k} = 0$, the need to ignore the interpolation step will not arise. In this new technique, the $D^1|_{i+0.5,j,k}$ component is calculated from equation 7.

$$E_1\big|_{i+0.5,j,k} = 0 = \frac{\mathbf{U}_1\big|_{i,j,k} \cdot \mathbf{U}_1\big|_{i,j,k}}{\varepsilon\sqrt{g}} D^1\big|_{i+0.5,j,k} + \left\{ \frac{\mathbf{U}_1\big|_{i,j,k} \cdot \mathbf{U}_3\big|_{i,j,k}}{4\varepsilon\sqrt{g}} D^3\big|_{i,j,k+0.5} + \frac{\mathbf{U}_1\big|_{i,j,k} \cdot \mathbf{U}_3\big|_{i+1,j,k}}{4\varepsilon\sqrt{g}} D^3\big|_{i+1,j,k+0.5} + \ldots\ldots\ldots\ldots \right\} \quad (7)$$

This technique will ensure the symmetry of the material matrices and hence the stability of the algorithm. The physical conditions required for a metallic boundary is also satisfied as the tangential covariant components are zero. However, contributions from field components on the metallic boundary such as $D^2|_{i,j+0.5,k}$, $D^2|_{i+1,j+0.5,k}$ must be set to zero as it will complicate the calculation of $D^1|_{i+0.5,j,k}$. Initial numerical analysis with this technique showed improvements on numerical errors, however the mesh still suffered numerical dispersion for very small cell sizes. These small errors may be due to the calculation of $D^1|_{i+0.5,j,k}$ being different from the main non-orthogonal FDTD algorithm (Equations 1-5). Adding extra weights to interpolation coefficients while maintaining symmetry in the calculation of $D^1|_{i+0.5,j,k}$ improved the results further. In this analysis, a weighting factor of 4/2.8 was employed to weight the interpolation coefficients. i.e. the:

$$\frac{\mathbf{U}_1\big|_{i,j,k} \cdot \mathbf{U}_3\big|_{i,j,k}}{4\varepsilon\sqrt{g}} \quad , \quad \frac{\mathbf{U}_1\big|_{i,j,k} \cdot \mathbf{U}_3\big|_{i+1,j,k}}{4\varepsilon\sqrt{g}}$$

terms in equation 4 were multiplied by this factor and the same value is then used in the calculation of the fields such as $E_3|_{i,j,k+0.5}$ to ensure stability. This factor was estimated by investigating different mesh structures. The following section numerically analyse these techniques using a Microstrip line and a patch antenna.

III. Numerical Analysis and Results

Figure 2 shows an air-spaced (non-dispersive) microstrip line which is used here to demonstrate the metallic boundary effect through an analysis of the numerical dispersion in the model [4].

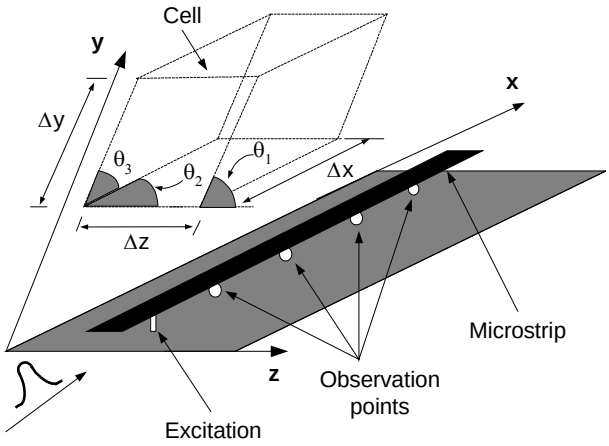

Figure 2: *Microstrip line and skewed cells.*

A Gaussian pulse of 200ps width was used to excite the problem and the electric fields were observed at four different locations. The microstrip line was made sufficiently long to avoid any influences from Mur's first order absorbing boundary conditions [7]. The interpolation step was ignored at the absorbing boundaries to avoid complexities arising due to non-orthogonal unit cells. The problem space was uniformly discretised into 140×25×40 unit cells, with a dimension of 6.5 mm in the longitudinal direction. As shown in Figure 2, the unit cells were distorted with either 2 or 3 angles of skew (θ_1, θ_2,. θ_3). The problem space was limited by employing absorbing boundaries and an electric wall to represent the ground plane.

The dispersion suffered by the pulse as it propagates through the model was calculated as described in [4]. Figure 3 and Figure 4 show the normalised wave numbers for meshes with $\theta_1=90^o$, $\theta_2=90^o$,. $\theta_3=45^o$ and $\theta_1=60^o$, $\theta_2=80^o$,. $\theta_3=50^o$ respectively. The simulation

results include the original technique, the proposed technique where $D^1|_{i+0.5,j,k} \neq 0$ and the incorporation of weighting factors.

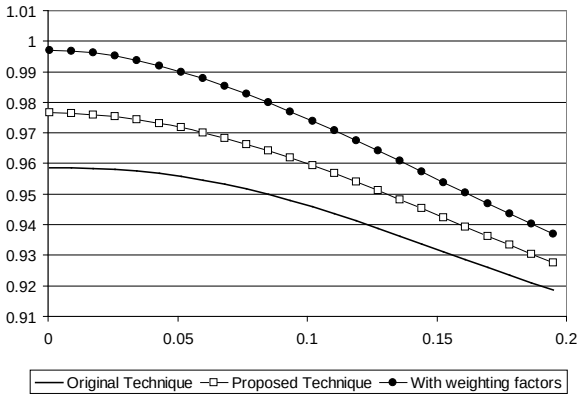

Figure 3: *Dispersive behaviour with one skew angle.*

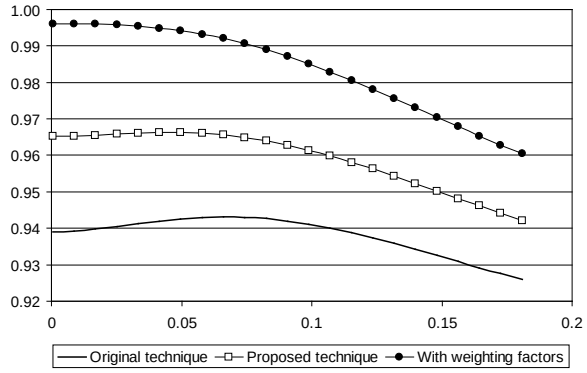

Figure 4: *Dispersive behaviour with three skew angles.*

Figure 5 shows a second test structure, an air-spaced microstrip patch antenna (50×40 mm, lying 3.2 mm above the ground plane); a dielectric substrate was not included in this structure in order to simplify the problem and to separate the errors due to the metallic boundary. As before, Mur's first-order absorbing condition was employed to limit the problem space. For simplicity, a feed is not included, the fields being excited and recorded directly on the antenna. A uniformly skewed mesh with $\theta_1=90^o$, $\theta_2=90^o$, $\theta_3=45^o$ as in Figure 2 was employed to analyse the patch antenna structure.

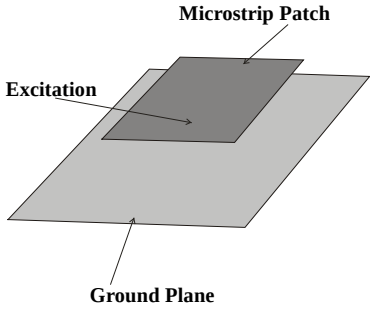

Figure 5: *Air-spaced microstrip patch antenna.*

Figure 6 shows a discrete Fourier transform (DFT) of the response of the patch. Simulation results include, fine orthogonal mesh, which provides a reference result, the original technique, proposed technique and the incorporation of the weighting factors.

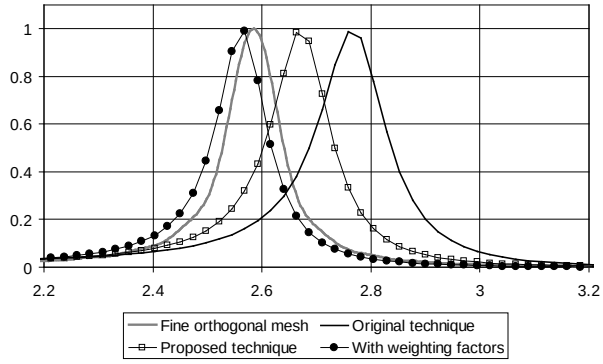

Figure 6: *Frequency response of the patch.*

These results clearly show the improvements when applying the proposed technique and the incorporation of the weighting factors. In Figure 6, the non-orthogonal algorithm with proposed technique and weighting factors produced a very accurate estimation of the patch resonance.

The numerical results from the two test structures in this section confirm that significant dispersive errors are introduced if, at a metallic boundaries on a non-orthogonal mesh, it is assumed that the covariant tangential electric field components and the couplings from their contravariant components are zero. As can be seen in Figures 3 and 4, the normalised wave numbers remain around 0.96 and 0.94 for the original technique. The alternative, suggested herein, is to calculate the contravariant components on the metallic surfaces while maintaining zero covariant components; this gives improved results in all cases and incorporation of weighting factors further improves the numerical errors.

V. Conclusions

The modelling of metallic boundaries using a non-orthogonal FDTD method has been presented. The difficulties in representing metallic boundaries have been described. The modelling of metal surfaces using non-orthogonal meshes by assuming that the covariant tangential electric field components, and the coupling from their contravariant components, is zero, results in significant errors leading to numerical dispersion.

An alternative technique where the calculation of contravariant components on the metallic surfaces while maintaining zero covariant components and non-zero coupling from other contravarient components has been presented. Numerical analyses using microstrip line and an air-spaced patch antenna showed improve results and the stability of the algorithm was also maintained. Further enhancement to the numerical errors was also achieved through incorporating weighting factors when

calculating the contravariant components on the metal surface.

In conclusion, while non-orthogonal meshes offer a solution to staircasing problems in FDTD, suitable correction techniques are required to limit the numerical dispersion even for very small cell sizes.

VII. References

[1] K. S. Yee, "Numerical solutions of initial boundary value problems involving Maxwell's equations in isotropic media", *IEEE Trans., Antennas and Prop.*, vol. 14, 1966, 302-307.

[2] T. G. Jurgens, A. Taflove, K. R. Umashankar, T. G. Moore, "Finite Difference Time Domain Modelling of Curved Surfaces", *IEEE Trans., Antennas and Prop.*, vol. 40, 1992, , 357-366

[3] R. Holland, "Finite-difference solution of Maxwell's equations in generalized nonorthogonal coordinates", *IEEE Trans. Nucl. Sci.*, vol. 30, 1983, 4586–459

[4] R. Nilavalan, I. J. Craddock and C. J. Railton, "Quantifying numerical dispersion in non-orthogonal FDTD meshes", *IEE Proceedings-Microwaves Antennas & Propagation*, vol. 149, 2002, 23-27

[5] R. Nilavalan, I. J. Craddock and C. J. Railton, "Modelling metallic discontinuities with the non-orthogonal FDTD method", *IEE Proceedings-Microwaves Antennas & Propagation*, vol. 151, 2004, 425-429.

[6] R. Schumann, and T. Weiland, "Stability of the FDTD algorithm on non-orthogonal grids related to the spatial interpolation scheme", *IEEE Trans. Magn.*, vol. 34, 1998, 2751–2754

[7] G. Mur, "Absorbing boundary conditions for the finite difference approximation of the time domain electromagnetic-field equations", *IEEE Trans. on Electromagnetic Compatibility*, 23, 1981, 377-382.